

## OBSTACLE AVOIDANCE CONTROL FOR TWO-WHEEL DIFFERENTIAL ROBOT USING POTENTIAL METHOD AND GESTURE

NAOYA NAKAZAWA<sup>1</sup>, KOICHI TOKAIRIN<sup>1</sup>, KOTARO HASHIKURA<sup>2</sup>  
TRINH TRUNG HIEU<sup>3</sup>, NGHIA THI MAI<sup>3</sup>, MD ABDUS SAMAD KAMAL<sup>2</sup>  
IWANORI MURAKAMI<sup>2</sup> AND KOU YAMADA<sup>2</sup>

<sup>1</sup>Graduate School of Science and Technology

<sup>2</sup>Division of Mechanical Science and Technology

Gunma University

1-5-1 Tenjincho, Kiryu 376-8515, Japan

{ t231b064; t201b064; k-hashikura; maskamal; murakami; yamada }@gunma-u.ac.jp

<sup>3</sup>Department of Electrical and Electronic 1

Posts and Telecommunications Institute of Technology

Km10, Nguyen Trai, Ha Dong District, Hanoi 151090, Vietnam

{ hieutt; nghiamt }@ptit.edu.vn

Received June 2023; accepted September 2023

**ABSTRACT.** *The potential method that is one of the obstacle avoidance control methods for robots is necessary to set appropriate parameters, since the avoidance path changes by adjusting the weight of the potential. In this paper, we propose a system that adjusts the weight of the repulsive potential by gesture. In addition, we present a path-following method for differential two-wheeled robots, which focuses on cooperation with the potential method. The proposed obstacle avoidance control by gesture operation can make the obstacle avoidance path smaller than the conventional path by lowering the weight of the repulsive potential by gesture operation while the robot is running. This proposed method gives us more freedom in the path and provides the generation of efficient obstacle paths.*

**Keywords:** Two-wheel differential robot, Potential method, Path-following method, Gesture

1. **Introduction.** Many studies on obstacle avoidance control have been published [1, 2, 3, 4, 5, 6, 7]. Obstacle control challenges include route inefficiency. This inefficiency can result from a variety of factors, and it is critical to address this inefficiency to improve the overall performance and effectiveness of robot navigation.

One of the obstacle avoidance control methods for robots is the potential method [5]. This method constructs a potential field by defining the attractive potential that moves the robot toward the goal position and the repulsive potential that moves the robot away from obstacle positions and generates the path of the robot from the gradient of the potential field. This method is possible to deal with unknown obstacles because the calculation of the potential functions changes the route in real time based on the observation information up to that point [6]. It is necessary to set appropriate parameters, since the avoidance path changes by adjusting the parameters [7]. Yashiro et al. [6] establish control logic added capabilities that update the list storing obstacle coordinate and adjust the weight of the potential field. This research enables the robot to move away from the obstacle temporarily by lowering the weight factor of the goal position while remembering the approaching obstacle in case of deadlock. After that, when the weight of the goal position

is restored again, the robot moves to the goal position while avoiding the stored obstacles. However, the robot takes a detour to avoid an obstacle once, which is not an efficient path.

In order to overcome these problems, Szczepanski et al. [13] and Dini and Saponara [14] propose a potential method using predictive control. In these methods, the robot's path is determined by the robot's position, the goal's position, the obstacle's position, and the size of the obstacle. However, when we want to change the robot's path while the robot is running, considering the situation like the size of the obstacles, these methods cannot do so. In other words, the person operating the robot at the site cannot change the robot's path, which has been determined, in real time.

In this paper, we propose an obstacle avoidance control method for a differential two-wheeled robot using a system that adjusts the weight of repulsive potential by gesture to reduce this path length. Gesture can be operated intuitively by body movement as [8, 9]. The proposed method provides the generation of efficient obstacle paths in real time. This paper is organized as follows. In Section 2, we introduce a mathematical model of the differential two-wheeled robot and the equation of motion of the two-wheeled robot driven by DC motors. In addition, we propose a path-following method for differential two-wheeled robots that focuses on cooperation with the potential method, and a gesture for controlling the weight of the repulsive potential. In Section 3, we conduct an obstacle avoidance simulation with the proposed gesture operation, compare the results when the weight of the repulsive potential is changed by the gesture and the result when the weight is constant, and show the effectiveness of this designed control. In Section 4, we give some concluding remarks.

## 2. Obstacle Avoidance Control Design for Two-Wheel Differential Robot.

In this section, we introduce a mathematical model of the differential two-wheeled robot and the equation of motion of the two-wheeled robot driven by DC motors. In addition, we propose a path-following method for differential two-wheeled robots that focuses on cooperation with the potential method, and a gesture for controlling the weight of the repulsive potential. We can freely change the weight of repulsive potential by gesture operations. That means we can move the path closer to or away from the obstacle and operate the robot as we wish; in other words, this proposed method gives us more freedom in the path and provides the generation of efficient obstacle paths.

The mathematical model of the differential two-wheeled robot is given in Figure 1 [11, 12]. This differential two-wheeled robot is assumed to have two wheels and be able to move on the floor by driving both wheels independently with a DC motor. Here,  $M$  [kg] is the vehicle body weight,  $r$  [m] is wheel radius,  $v$  [m/s] is the translational velocity,  $\omega$  [rad/s] is the rotational velocity,  $v_R$  [m/s] and  $v_L$  [m/s] are the velocity of the right and left wheels, respectively, and  $L$  [m] is distance between wheels.

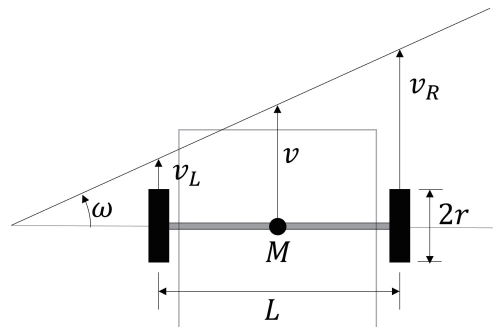


FIGURE 1. Mathematical model of two-wheel differential robot

The translational velocity  $v$  and rotational velocity  $\omega$  of the differential two-wheeled robot are given by

$$v = \frac{v_R + v_L}{2} \quad (1)$$

and

$$\omega = \frac{v_R - v_L}{L}, \quad (2)$$

respectively.

The equation of motion of a two-wheeled robot in Figure 1 driven by a DC motor can be expressed by

$$\begin{aligned} & \begin{bmatrix} \frac{Mr^2}{4} + \frac{Ir^2}{L} + J & \frac{Mr^2}{4} - \frac{Ir^2}{L} \\ \frac{Mr^2}{4} - \frac{Ir^2}{L} & \frac{Mr^2}{4} + \frac{Ir^2}{L} + J \end{bmatrix} \begin{bmatrix} \ddot{\theta}_R(t) \\ \ddot{\theta}_L(t) \end{bmatrix} \\ = & \begin{bmatrix} \frac{-n^2K_bK_t}{R_m} & 0 \\ 0 & \frac{-n^2K_bK_t}{R_m} \end{bmatrix} \begin{bmatrix} \dot{\theta}_R(t) \\ \dot{\theta}_L(t) \end{bmatrix} + \begin{bmatrix} \frac{nK_t}{R_m} & 0 \\ 0 & \frac{nK_t}{R_m} \end{bmatrix} \begin{bmatrix} u_R(t) \\ u_L(t) \end{bmatrix}. \end{aligned} \quad (3)$$

Here,  $I$  [kgm<sup>2</sup>] is vehicle body inertia moment,  $J$  [kgm<sup>2</sup>] is sum of wheel inertia moment and DC motor inertia constant,  $K_b$  [kgm<sup>2</sup>] is DC motor back electro motive force (EMF) constant,  $K_t$  [Nm/A] is DC motor torque constant,  $R_m$  [ $\Omega$ ] is DC motor resistance,  $n$  is gear ratio,  $[\theta_R(t) \ \theta_L(t)]^T$  are wheel angles and  $[u_R(t) \ u_L(t)]^T$  are motor input voltages.

We settle the output of the system as  $[v \ \omega]^T$ . From Equations (1), (2) and (3), the equations of motion of the motors are expressed in state-space representation as

$$\begin{cases} \begin{bmatrix} \ddot{\theta}_R(t) \\ \ddot{\theta}_L(t) \end{bmatrix} = A_v \begin{bmatrix} \dot{\theta}_R(t) \\ \dot{\theta}_L(t) \end{bmatrix} + B_v \begin{bmatrix} u_1(t) \\ u_2(t) \end{bmatrix} \\ \begin{bmatrix} v(t) \\ \omega(t) \end{bmatrix} = C_v \begin{bmatrix} \dot{\theta}_R(t) \\ \dot{\theta}_L(t) \end{bmatrix} \end{cases}, \quad (4)$$

where

$$A_v = \begin{bmatrix} \frac{Mr^2}{4} + \frac{Ir^2}{L} + J & \frac{Mr^2}{4} - \frac{Ir^2}{L} \\ \frac{Mr^2}{4} - \frac{Ir^2}{L} & \frac{Mr^2}{4} + \frac{Ir^2}{L} + J \end{bmatrix}^{-1} \begin{bmatrix} \frac{-n^2K_bK_t}{R_m} & 0 \\ 0 & \frac{-n^2K_bK_t}{R_m} \end{bmatrix}, \quad (5)$$

$$B_v = \begin{bmatrix} \frac{Mr^2}{4} + \frac{Ir^2}{L} + J & \frac{Mr^2}{4} - \frac{Ir^2}{L} \\ \frac{Mr^2}{4} - \frac{Ir^2}{L} & \frac{Mr^2}{4} + \frac{Ir^2}{L} + J \end{bmatrix}^{-1} \begin{bmatrix} \frac{nK_t}{R_m} & 0 \\ 0 & \frac{nK_t}{R_m} \end{bmatrix} \quad (6)$$

and

$$C_v = \begin{bmatrix} \frac{r}{2} & \frac{r}{2} \\ \frac{r}{L} & -\frac{r}{L} \end{bmatrix}. \quad (7)$$

### 2.1. Path-following method focusing on coordination with potential method.

The potential method constructs a potential field by defining the attractive potential that moves the robot toward the goal position and the repulsive potential that moves the robot away from obstacle positions, and generates the path of the robot from the gradient of the potential field [6].

The attractive potential  $P_g(x, y)$  that moves the robot toward the goal is defined by

$$P_g(x, y) = \frac{1}{\sqrt{(x - x_g)^2 + (y - y_g)^2}}, \quad (8)$$

where  $[x \ y]^T$  is robot position and  $[x_g \ y_g]^T$  is goal position.

The repulsive potential  $P_o(x, y)$  that moves the robot away from obstacles is defined by

$$P_o(x, y) = -\frac{1}{\sqrt{(x - x_o)^2 + (y - y_o)^2}}, \quad (9)$$

where  $[x_o \ y_o]^T$  is obstacle position.

Using above, the overall potential function  $P(x, y)$  is defined by

$$P(x, y) = w_g P_g + w_o P_o, \quad (10)$$

where  $w_g$  is the weight of the attractive potential created by the goal, which means the magnitude of the attractive force, and  $w_o$  is the weight of the repulsive potential created by the obstacle, and means the magnitude of the repulsive force.

The potential gradient can be expressed as

$$-\nabla P(x, y) = -\left[ \frac{\partial P}{\partial x} \quad \frac{\partial P}{\partial y} \right]^T. \quad (11)$$

Equation (11) shows a direction away from obstacles and approaching the goal position. The robot can move to the goal position while avoiding obstacles, using this gradient as the moving direction at that time [6]. We consider the path-following method that uses the potential gradient as shown in Figure 2. Here,  $q$  [m] is the magnitude of direction from the robot position up to goal position and  $\phi$  [rad] is a direction from the robot position up to goal position.

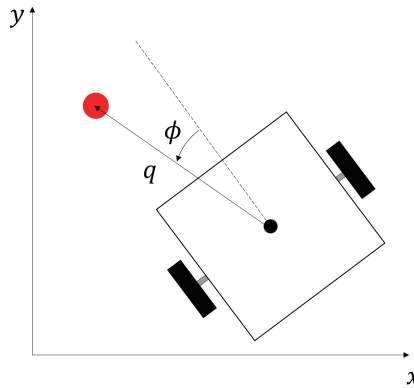


FIGURE 2. Path-following method with potential method overview

The magnitudes of direction  $q$  [m] and direction  $\phi$  [rad] from the robot position up to goal position as seen from the robot are written by

$$q = \sqrt{\left\{ \frac{-\frac{\partial P}{\partial x}}{\|\nabla P\|} \right\}^2 + \left\{ \frac{-\frac{\partial P}{\partial y}}{\|\nabla P\|} \right\}^2} \quad (12)$$

and

$$\phi = \arctan 2 \{R(1, 2), R(1, 1)\}, \quad (13)$$

where  $\arctan 2$  is two-variable inverse tangent function and defined by

$$\arctan 2(b, a) = \begin{cases} \arctan(b, a) & (a > 0) \\ \arctan(b, a) + \pi & (a < 0, b > 0) \\ \arctan(b, a) - \pi & (a < 0, b < 0) \\ +\frac{\pi}{2} & (a = 0, b > 0) \\ -\frac{\pi}{2} & (a = 0, b < 0) \\ \text{undefined} & (a = 0, b = 0) \end{cases}, \quad (14)$$

and  $R$  is the potential gradient multiplied by the rotation matrix around the  $z$  axis and given by

$$R = \begin{bmatrix} \cos \theta & -\sin \theta \\ \sin \theta & \cos \theta \end{bmatrix} [ -\nabla P ]. \quad (15)$$

In addition, using Equations (12) and (13), it calculates the control amount required by the robot, that is, the command translational velocity and command rotational velocity. Then, we need to control them according to our purpose. Feedback needs to reduce the deviation between the robot position and the goal position because the robot moves on a plane. Then the robot will change its direction according to the angle toward the goal position. There exists control method to reduce the deviation between the robot position and the goal position, which is the gain feedback control described in [10]. Therefore, we adapt the gain feedback control. The translational velocity  $v$  and the velocity difference  $\Delta v$  between right wheel and left wheel can be expressed by

$$v = K_q q \quad (16)$$

and

$$\Delta v = K_\phi \phi, \quad (17)$$

respectively. The velocity of the right  $v_R$  and left  $v_L$  wheels can be expressed by

$$\begin{cases} v_R = v + \Delta v \\ v_L = v - \Delta v \end{cases}. \quad (18)$$

Using above, we can convert to translational velocity  $v$  and rotational velocity  $\omega$  by Equations (1) and (2), and sent to the motor as command values.

**2.2. Gesture for controlling the weight of the repulsive potential.** In this subsection, we describe a gesture operation that controls the weight  $w_o$  of the repulsive potential. We adopt a swipe Graphical User Interface (GUI) system [11] shown in Figure 3. In this system, a human stands in front of the camera and uses a pen-style input device shown in Figure 3 to make a swipe motion. The RGB camera captures the light-emitting part from the input device, and binaries and morphologically processes the distortion of the object to extract a rough object. Then, the position is estimated from the changes in those features, and the input for the gesture operation is generated from the device state at that time and the device state one step before.

According to [11], this system can effectively follow human gestures that require quick changes and high-speed input such as swipe motion. The robot's goal point is generated by gesture operation.

In contrast, the weight is controlled by gesture operation. We designed a system shown in Figure 4 in which moving the device to the right increases the weight  $w_o$  of the repulsive potential, and moving the device to the left decreases  $w_o$ .

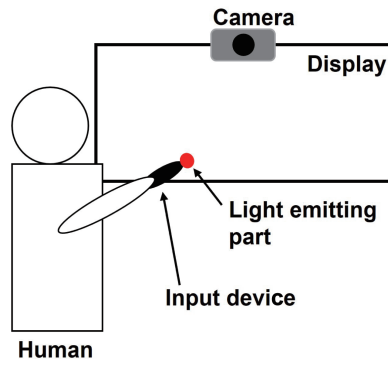


FIGURE 3. GUI system overview [11]

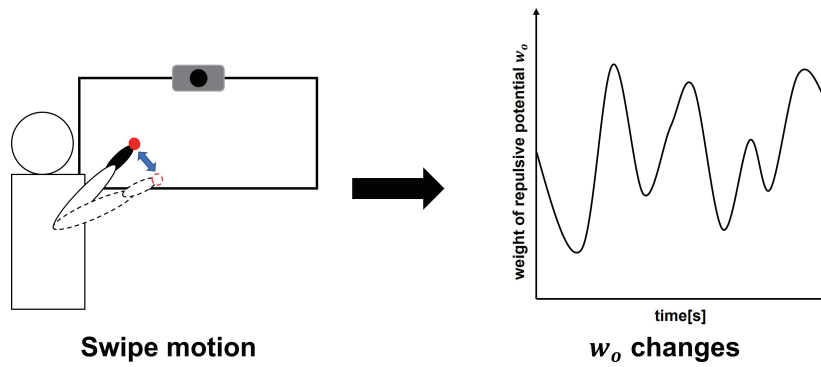


FIGURE 4. Swipe motion

**3. Control Experiments.** Obstacle avoidance simulation is conducted when the proposed gesture operation changed the weight  $w_o$  of the repulsive potential. As a conventional method, an obstacle avoidance simulation was conducted when the weight of the repulsive potential was constant ( $w_o = 1.0$ ).

The simulation results are shown in Figure 5. In Figure 5(a), the square is an obstacle, the solid line shows the resultant robot's paths using the proposed method and the dotted line shows those using conventional method. The robot moves from left to right. Figure 5(b) shows that the weight  $w_o$  of the repulsive potential changes with time by gesture operation in the case of the proposed method.

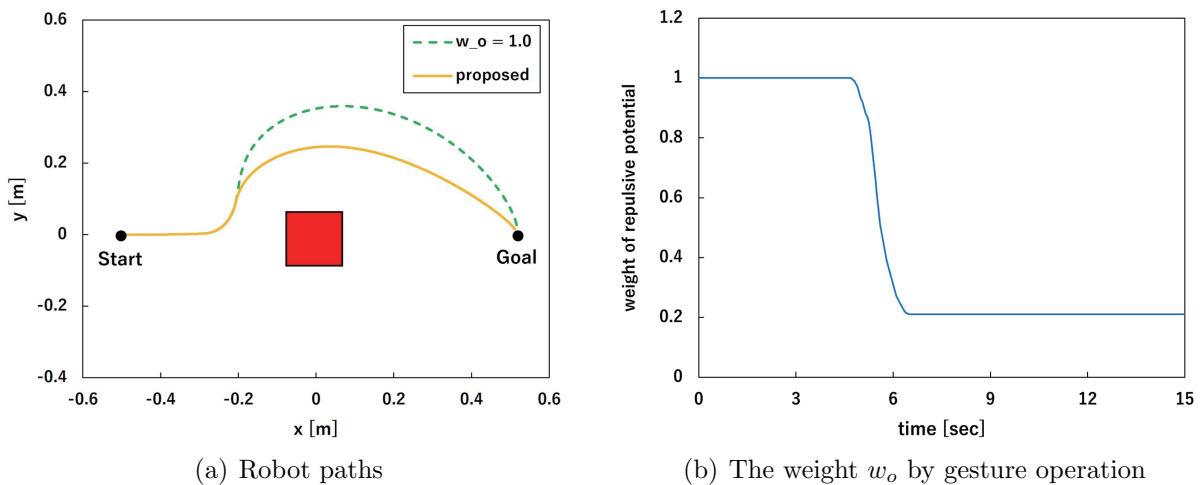


FIGURE 5. The simulation results

It is confirmed that the proposed method can change the path from the conventional path and make the robot's path smaller by lowering the weight  $w_o$  of the repulsive potential by gesture operation from 5 to 7 seconds in Figure 5(b). However, the timing of lowering  $w_o$  for gesture operation is important. This path can be made smaller by gesturing, when the robot starts to avoid the obstacle.

In this result, we can freely change the weight of repulsive potential by gesture operations. That is, we can move the path closer to or away from the obstacle and operate the robot as we wish; in other words, this proposed method gives us more freedom in the path. However, since the degree of freedom depends on the potential weights, appropriate weights must be set. Furthermore, since this method is performed using gesture operations, it is not autonomous driving. To create an autonomous mobile robot, an algorithm that changes the potential weight depending on the situation is required, and this is a future task.

**4. Conclusions.** In this paper, we have proposed obstacle avoidance control of the differential two-wheeled robot using potential method and gesture. We confirmed that the proposed obstacle avoidance control by gesture operation can make the obstacle avoidance path smaller than the conventional path by lowering the weight of the repulsive potential by gesture operation while the robot is running, showing efficacy. In the future, we will conduct experiments on how to place the weight of the repulsive potential on obstacles and achieve the realization of more suitable and autonomous obstacle avoidance considering the dynamic characteristics of the robot.

**Acknowledgment.** This research is supported by the Japan Society for the Promotion of Science (JSPS) Grant-in-Aid for Scientific Research (C) 23K03898 and JP21K03930.

#### REFERENCES

- [1] S. Aoyagi, N. Sato, K. Yamamoto, T. Takahashi and M. Suzuki, Learning of fuzzy rules for avoidance of a moving obstacle in a mobile robot-comparison with potential method and reinforcement learning method, *Journal of the Institute of Systems, Control and Information Engineers (ISCIE)*, vol.34, no.8, pp.209-218, 2021 (in Japanese).
- [2] S. Horiuchi, R. Hirano, K. Okada and S. Nohtomi, Optimal steering and breaking control in emergency obstacle avoidance, *Transactions of the JSME*, vol.72, no.722, pp.3250-3255, 2006 (in Japanese).
- [3] J. Jin and W. Chung, Obstacle avoidance control of two-wheel differential robots considering the uncertainty of the basis of encoder odometry information, *Sensors*, vol.19, no.2, 289, DOI: 10.3390/s19020289, 2019.
- [4] Y. Sakai and M. Kitazawa, Automated vehicle operation characteristics with overhead view monitoring, *Transactions of the JSME*, vol.62, no.601, pp.3508-3515, 1996 (in Japanese).
- [5] K. Sato, Global motion planning using a Laplacian potential field, *Journal of the Robotics Society of Japan*, vol.11, no.5, pp.702-709, 1993 (in Japanese).
- [6] Y. Yashiro, K. Eguchi, S. Iwasaki, Y. Yamauchi and M. Nakata, Development of obstacle avoidance control for robotic products using potential field, *Mitsubishi Heavy Industries Technical Review*, vol.51, no.1, pp.34-39, 2014.
- [7] H. Hashimoto, Y. Kunii, F. Harashima, V. I. Utkin and S. V. Drakunov, Obstacle avoidance control of multi-degree-of-freedom manipulator using electrostatic potential field and sliding mode, *Journal of the Robotics Society of Japan*, vol.11, no.8, pp.1220-1228, 1993 (in Japanese).
- [8] A. Namiki, Y. Sugahara and A. Matsuzaki, Development of investigation problem for mathematical modelling in control of robot by gesture: Linking between LEGO MINDSTORMS EV3 and Kinect for windows and focus on functions of ICT, *JSSE Reserch Report*, vol.32, no.7, pp.43-48, 2018 (in Japanese).
- [9] Y. Kuno, Body actions as pointing device, *IPSJ Transactions on Computer Vision and Image Media*, vol.43, no.4, pp.43-53, 2002 (in Japanese).
- [10] C. Gerald and F. Zhang, *Mobile Robots: Navigation, Control and Sensing, Surface Robots and AUVs*, Wiley-IEEE Press, 2020.

- [11] K. Toukairin, D. Koyama, K. Hashikura, M. A. S. Kamal and K. Yamada, Swipe gesture robotics system based on image processing and servo compensation, *2021 IEEE International Conference on Mechatronics and Automation (ICMA)*, pp.1082-1087, 2021.
- [12] M. Isobe, K. Hashikura, A. Kojima, M. A. S. Kamal and K. Yamada, Two-degree-of-freedom  $H^2$  output regulation with application to vehicle motion control, *2019 IEEE Vehicle Power and Propulsion Conference (VPPC)*, pp.1-6, 2019.
- [13] R. Szczepanski, T. Tarczewski and K. Erwinski, Energy efficient local path planning algorithm based on predictive artificial potential field, *IEEE Access*, vol.10, pp.39729-39742, 2022.
- [14] P. Dini and S. Saponara, Energy processor-in-the-loop validation of a gradient descent-based model predictive control for assisted driving and obstacles avoidance applications, *IEEE Access*, vol.10, pp.67958-67974, 2022.